Vol 10 No 4, April 2001
1009-1963/2001/10(04)/0300-07

Chinese Physics

© 2001 Chin. Phys. Soc.
and IOP Publishing Ltd

ABSORPTION PROPERTIES OF A DRIVEN FOUR-LEVEL DOPPLER-BROADENED SYSTEM

YUAN SHI (袁 石), WU JIN-HUI (吴金辉), and GAO JIN-YUE (高锦岳)
Department of Physics, Jilin University, Changchun 130023, *China*

(Received 27 July 2000)

This paper deals with the absorption spectra of a weak probe in a four-level Doppler-broadened system driven by three coherent fields. The main aim is to extend earlier studies of the spontaneous emission spectrum and to present a comprehensive survey of the spectral features of this system. In addition to a derivation of exact formulae for the spectra, we give an explanation with the help of an appropriate set of dressed atomic states. We also get a deeper insight into the physical origin of gain in view of the existence of a population inversion between the levels of the lasing transition. Finally, we explore the effect of Doppler broadening on the absorption profile of the weak probe.

Keywords: quantum coherence, absorption spectrum, dressed atomic states, Doppler broadening
PACC: 4250

I. INTRODUCTION

The study of spectral properties in a multi-level atom system has been a focus of quantum optics research since the 1970s.[1−4] Following the recent advances in the construction of atomic traps[5] and the direct observation of emission and absorption of individual quanta from isolated atoms,[6] it is again an interesting field.[7−10]

In a recent paper,[11] we proposed that the fluorescence spectrum of a driven four-level system can undergo significant changes when a third driving field is added to the model. The modifications affect most significantly the total radiated intensity and the linewidths of its spectral components; the linewidths, in particular, become a mixture of the individual atomic-decay parameters with weight factors that depend on the strength of the applied fields.

In this paper, we focus on the absorption properties of the four-level atom driven by three optical fields. The physical setting of interest is the same as that of Ref.[11], aside from the fact that the pumping mechanism has been ignored. For this reason, we limit our presentation to a sketch of the procedure and a description of the results, in the interest of providing an insight into the effect of the driving fields.

The system is illustrated schematically in Fig.1, which includes three driving fields Ω_0, Ω_1 and Ω_2 and the remaining spontaneous decay processes at the rates γ_1, γ_2, γ_3, γ_4 and γ_5.

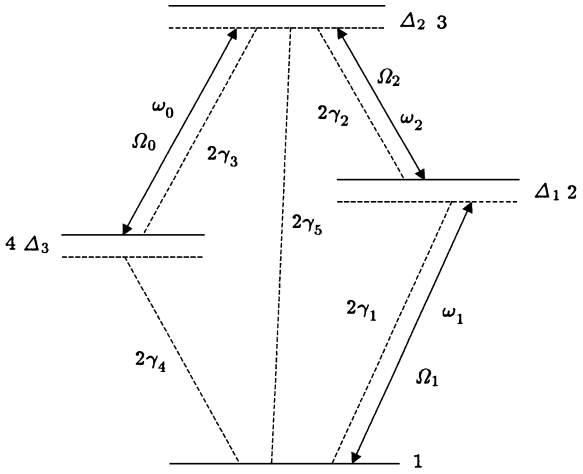


Fig.1. Schematic representation of the four-level model. $\Omega_0(\omega_0)$, $\Omega_1(\omega_1)$ and $\Omega_2(\omega_2)$ are the Rabi frequencies (carrier frequencies) of the driving fields. The Δ_1, Δ_2, Δ_3 and γ_1, γ_2, γ_3, γ_4, γ_5 are respectively detuning parameters and spontaneous decay rates.

The main task of this work is the derivation of exact formulae for the absorption spectra. Our results are valid for arbitrary strengths of the driving fields and the generalization of the resonance absorption spectra of a two-level or three-level system to the four-level system.

This paper is organized as follows. In section II we derive the equations of motion and analyse the absorption spectra. Section III is dedicated to a survey of the spectral results and the comparison of various predictions for different atomic configurations and gives an insight into the physical origin of the gain. In this section, we also discuss the effect of Doppler broadening on the absorption features of selected transitions.

II. CALCULATION OF THE SPECTRA

Following the procedure adopted in Ref.[11], our program is carried out as follows. Firstly, we derive the master equation for the four-level system in the semiclassical approximation, i.e., under the assumption that the three driving fields can be described by c-number functions. Next, we take advantage of the fact that the scattered electromagnetic field in the far zone is proportional to the atomic polarization operator for calculating the field correlation function and the spectrum of the emitted radiation. The absorption spectra require knowledge of the expected values of products of operators calculated at different times; we handle these quantities with the help of the quantum regression theorem.

The Hamiltonian of the four-level system interacting with three classical fields is given by

$$\begin{aligned} H =&\hbar\omega_{21}|2\rangle\langle 2| + \hbar(\omega_{32}+\omega_{21})|3\rangle\langle 3| + \hbar\omega_{41}|4\rangle\langle 4| \\ &+ \hbar\Omega_1|2\rangle\langle 1|\mathrm{e}^{-\mathrm{i}\omega_1 t} + \hbar\Omega_1^*|1\rangle\langle 2|\mathrm{e}^{\mathrm{i}\omega_1 t} \\ &+ \hbar\Omega_2|3\rangle\langle 2|\mathrm{e}^{-\mathrm{i}\omega_2 t} + \hbar\Omega_2^*|2\rangle\langle 3|\mathrm{e}^{\mathrm{i}\omega_2 t} \\ &+ \hbar\Omega_0|3\rangle\langle 4|\mathrm{e}^{-\mathrm{i}\omega_0 t} + \hbar\Omega_0^*|4\rangle\langle 3|\mathrm{e}^{\mathrm{i}\omega_0 t}, \end{aligned} \tag{1}$$

where ω_{21}, ω_{31} and ω_{41} are the atomic transition frequencies. Ω_0, Ω_1 and Ω_2 are the Rabi frequencies of the driving fields.

The interaction Hamiltonian in the interaction representation takes the form

$$\begin{aligned} H_{\mathrm{I}} =& -\hbar\Delta_1|2\rangle\langle 2| - \hbar(\Delta_1+\Delta_2)|3\rangle\langle 3| \\ &+ \hbar(\Delta_3-\Delta_1-\Delta_2)|4\rangle\langle 4| \\ &+ \hbar\Omega_1|2\rangle\langle 1| + \hbar\Omega_1^*|1\rangle\langle 2| \\ &+ \hbar\Omega_2|3\rangle\langle 2| + \hbar\Omega_2^*|2\rangle\langle 3| \\ &+ \hbar\Omega_0|3\rangle\langle 4| + \hbar\Omega_0^*|4\rangle\langle 3|, \end{aligned} \tag{2}$$

where

$$\Delta_1 = \omega_1 - \omega_{21}, \Delta_2 = \omega_2 - \omega_{32}, \Delta_3 = \omega_0 - \omega_{34}. \tag{3}$$

The master equation for an arbitrary multi-level system is

$$\frac{\partial\rho}{\partial t} = -\frac{\mathrm{i}}{\hbar}[H_{\mathrm{I}},\rho] + \Lambda\rho. \tag{4}$$

The relevant equation of motion for the matrix elements of the density operator (in the interaction representation) can be written in the form

$$\frac{\partial\Psi}{\partial t} = L\Psi + I, \tag{5}$$

where

$$\Psi_1=\rho_{12},\ \Psi_2=\rho_{13},\ \Psi_3=\rho_{14},\ \Psi_4=\rho_{21},\ \Psi_5=\rho_{22},\ \Psi_6=\rho_{23},\ \Psi_7=\rho_{24},\ \Psi_8=\rho_{31}, \tag{6a}$$

$$\Psi_9=\rho_{32},\quad \Psi_{10}=\rho_{33},\quad \Psi_{11}=\rho_{34},\quad \Psi_{12}=\rho_{41},\quad \Psi_{13}=\rho_{42},\quad \Psi_{14}=\rho_{43},\quad \Psi_{15}=\rho_{44}. \tag{6b}$$

The matrix L has the explicit form

$$L_{11}=-\mathrm{i}\Delta_1-\gamma_1,\quad L_{12}=\mathrm{i}\Omega_2,\quad L_{15}=-2\mathrm{i}\Omega_1^*,\quad L_{10}=-\mathrm{i}\Omega_1^*,\quad L_{115}=-\mathrm{i}\Omega_1^*, \tag{7a}$$

$$L_{21}=\mathrm{i}\Omega_2^*,\quad L_{22}=-\mathrm{i}(\Delta_1+\Delta_2)-\gamma_2-\gamma_3-\gamma_5,\quad L_{23}=\mathrm{i}\Omega_0^*,\quad L_{26}=-\mathrm{i}\Omega_1^*, \tag{7b}$$

$$L_{32}=\mathrm{i}\Omega_0,\quad L_{33}=-\mathrm{i}(\Delta_1+\Delta_2-\Delta_3)-\gamma_4,\quad L_{37}=-\mathrm{i}\Omega_1^*, \tag{7c}$$

$$L_{44}=\mathrm{i}\Delta_1-\gamma_1,\quad L_{45}=2\mathrm{i}\Omega_1,\quad L_{48}=-i\Omega_2^*,\quad L_{410}=\mathrm{i}\Omega_1,\ L_{415}=\mathrm{i}\Omega_1, \tag{7d}$$

$$L_{51}=-\mathrm{i}\Omega_1,\quad L_{54}=\mathrm{i}\Omega_1^*,\quad L_{55}=-2\gamma_1,\quad L_{56}=\mathrm{i}\Omega_2,\quad L_{59}=-\mathrm{i}\Omega_2^*,\quad L_{510}=2\gamma_2, \tag{7e}$$

$$L_{62}=-\mathrm{i}\Omega_1,\quad L_{65}=\mathrm{i}\Omega_2^*,\quad L_{66}=-\mathrm{i}\Delta_2-\gamma_1-\gamma_2-\gamma_3-\gamma_5,\quad L_{67}=\mathrm{i}\Omega_0^*,\quad L_{610}=-\mathrm{i}\Omega_2^*, \tag{7f}$$

$$L_{73}=-\mathrm{i}\Omega_1,\quad L_{76}=\mathrm{i}\Omega_0,\quad L_{77}=-\mathrm{i}(\Delta_2-\Delta_3)-\gamma_1-\gamma_4,\quad L_{711}=-\mathrm{i}\Omega_2^*, \tag{7g}$$

$$L_{84}=-\mathrm{i}\Omega_2,\quad L_{88}=\mathrm{i}(\Delta_1+\Delta_2)-\gamma_2-\gamma_3-\gamma_5,\quad L_{89}=\mathrm{i}\Omega_1,\quad L_{812}=-\mathrm{i}\Omega_0, \tag{7h}$$

$$L_{95}=-\mathrm{i}\Omega_2,\quad L_{98}=\mathrm{i}\Omega_1^*,\quad L_{99}=\mathrm{i}\Delta_2-\gamma_1-\gamma_2-\gamma_3-\gamma_5,\quad L_{910}=\mathrm{i}\Omega_2^*,\quad L_{913}=-\mathrm{i}\Omega_0, \tag{7i}$$

$$L_{106}=-\mathrm{i}\Omega_2,\quad L_{109}=\mathrm{i}\Omega_2^*,\quad L_{1010}=-2\gamma_2-2\gamma_3-2\gamma_5,\quad L_{1011}=\mathrm{i}\Omega_0^*,\quad L_{1014}=-\mathrm{i}\Omega_0, \tag{7j}$$

$$L_{117}=-\mathrm{i}\Omega_2,\quad L_{1110}=\mathrm{i}\Omega_0,\quad L_{1111}=\mathrm{i}\Delta_3-\gamma_2-\gamma_3-\gamma_4-\gamma_5,\quad L_{1115}=-\mathrm{i}\Omega_0, \tag{7k}$$

$$L_{128}=-\mathrm{i}\Omega_0^*,\quad L_{1212}=\mathrm{i}(\Delta_1+\Delta_2-\Delta_3)-\gamma_4,\quad L_{1213}=\mathrm{i}\Omega_1, \tag{7l}$$

$$L_{139}=-\mathrm{i}\Omega_0^*,\quad L_{1312}=\mathrm{i}\Omega_1^*,\quad L_{1313}=\mathrm{i}(\Delta_2-\Delta_3)-\gamma_1-\gamma_4,\quad L_{1314}=\mathrm{i}\Omega_2, \tag{7m}$$

$$L_{1410}=-\mathrm{i}\Omega_0^*,\quad L_{1413}=\mathrm{i}\Omega_2^*,\quad L_{1414}=-\mathrm{i}\Delta_3-\gamma_2-\gamma_3-\gamma_4-\gamma_5,\quad L_{1415}=\mathrm{i}\Omega_0^*, \tag{7n}$$

$$L_{1510}=2\gamma_3,\quad L_{1511}=-\mathrm{i}\Omega_0^*,\quad L_{1514}=\mathrm{i}\Omega_0,\quad L_{1515}=-2\gamma_4, \tag{7o}$$

where γ_i and Δ_i are the corresponding spontaneous decay rates and detuning parameters, respectively.

The inhomogeneous vector I has nonzero components

$$I_1 = \mathrm{i}\Omega_1^*, \quad I_4 = -\mathrm{i}\Omega_1. \tag{8}$$

The four-level system is driven by the external fields at frequencies ω_1, ω_2 and ω_0, and is probed by a tunable weak beam whose attenuation (or amplification) is measured in transmission. According to the linear-response theory[12] the exponential attenuation coefficient at a given frequency ω is given by

$$A(\omega) = \text{const} \times \xi\{\langle [P^{(-)}(\tau_1), P^{(+)}(\tau_0)]\rangle\}, \tag{9}$$

where ξ denotes the Fourier transform operator. The square brackets indicate the unequal time commutator and the quantum ensemble average $\langle\ \rangle$ must be carried out under steady-state conditions, i.e., in the limit $t_0, t_1 \to \infty$.

The absorption spectrum is composed of two parts: the first, $\langle P^{(-)}(\tau_1)P^{(+)}(\tau_0)\rangle$, is identical to the one calculated in Ref.[11]; the second, $\langle P^{(+)}(\tau_0)P^{(-)}(\tau_1)\rangle$, can be derived following the same procedure with minor modifications. The starting point in Laplace space is the single-time average

$$\begin{aligned}\langle p^{(-)}(z)\rangle =& \mu_{41}\,\Phi_3(z_1) + \mu_{21}\,\Phi_1(z_2) + \mu_{31}\,\Phi_2(z_3) \\ &+ \mu_{32}\,\Phi_6(z_4) + \mu_{34}\,\Phi_{14}(z_5).\end{aligned} \tag{10}$$

Here we give an example for the calculation of the absorption spectrum for the transmission $1 \to 4$

$$\begin{aligned}&\langle p^{(+)}(\infty)P^{(-)}(z)\rangle \\ =&\mu_{41}\mu_{14}\Big(M_{33}(1 - \Psi_5 - \Psi_{10} - \Psi_{15}) + M_{37}\,\Psi_4 \\ &+ M_{311}\,\Psi_8 + M_{315}\,\Psi_{12} + \frac{1}{z}\sum_{j=1}^{15} M_{3j}I_j\,\Psi_{12}\Big),\end{aligned} \tag{11}$$

$$\begin{aligned}&\langle [p^{(-)}(z), P^{(+)}(\tau_0)]\rangle \\ =&\mu_{41}\mu_{14}(M_{31}\,\Psi_{13} + M_{32}\,\Psi_{14} \\ &+ M_{33}(2\,\Psi_{15} - 1 + \Psi_5 + \Psi_{10}) \\ &- M_{37}\,\Psi_4 - M_{311}\,\Psi_8 - M_{315}\,\Psi_{12}).\end{aligned} \tag{12}$$

A similar expression holds for the remaining expectation values. The complete expression of the absorption spectrum (in Laplace space) is given by

$$\begin{aligned}&\langle [p^{(-)}(z), P^{(+)}(\tau_0)]\rangle \\ =&\mu_{41}\mu_{14}(M_{31}(z_1)\,\Psi_{13} + M_{32}(z_1)\,\Psi_{14} \\ &+ M_{33}(z_1)(2\,\Psi_{15} - 1 + \Psi_5 + \Psi_{10}) \\ &- M_{37}(z_1)\,\Psi_4 - M_{311}(z_1)\,\Psi_8 - M_{315}(z_1)\,\Psi_{12}) \\ &+ \mu_{21}\mu_{12}(M_{11}(z_2)(2\,\Psi_5 - 1 + \Psi_{10} + \Psi_{15}) \\ &+ M_{12}(z_2)\,\Psi_6 + M_{13}(z_2)\,\Psi_7 \\ &- M_{15}(z_2)\,\Psi_4 - M_{19}(z_2)\,\Psi_8 - M_{113}(z_2)\,\Psi_{12}) \\ &+ \mu_{31}\mu_{13}(M_{21}(z_3)\,\Psi_9 \\ &+ M_{22}(z_3)(2\,\Psi_{10} - 1 + \Psi_5 + \Psi_{15}) \\ &+ M_{23}(z_3)\,\Psi_{11} - M_{26}(z_3)\,\Psi_4 \\ &- M_{210}(z_3)\,\Psi_8 - M_{214}(z_3)\,\Psi_{12}) \\ &+ \mu_{32}\mu_{23}(M_{64}(z_4)\,\Psi_8 + M_{65}(z_4)\,\Psi_9 + M_{66}(z_4)\,\Psi_{10} \\ &+ M_{67}(z_4)\,\Psi_{11} - M_{62}(z_4)\,\Psi_1 - M_{66}(z_4)\,\Psi_5 \\ &- M_{610}(z_4)\,\Psi_9 - M_{614}(z_4)\,\Psi_{13}) \\ &+ \mu_{34}\mu_{43}(M_{1412}(z_5)\,\Psi_8 \\ &+ M_{1413}(z_5)\,\Psi_9 + M_{1414}(z_5)\,\Psi_{10} \\ &+ M_{1415}(z_5)\,\Psi_{11} - M_{142}(z_5)\,\Psi_3 - M_{146}(z_5)\,\Psi_7 \\ &- M_{1410}(z_5)\,\Psi_{11} - M_{1414}(z_5)\,\Psi_{15}),\end{aligned} \tag{13}$$

and

$$A(\omega) = \mathrm{Re}\langle [P^{(-)}(z), P^{(+)}(\tau_0)]\rangle_{z=i(\omega-\omega_1-\omega_2+\omega_0)}, \tag{14}$$

$$\Psi_i(\infty) = -\sum_{j=1}^{15}(L^{-1})_{ij}I_j, \tag{15}$$

$$M_{ij}(z) = [(z - L)^{-1}]_{ij}. \tag{16}$$

III. A SURVEY OF THE NUMERICAL RESULTS

This section contains a graphical survey of some specific predictions that emerge from the formulae derived in section II. In the calculations, we scale all the detuning parameters and field Rabi frequencies in terms of γ_4. We find there can be striking differences between the absorption spectra produced by an atom driven by two (one) or three resonant fields. Here we give an example for the absorption spectra of the $1 \to 4$ transition. Firstly, we consider the situation that only one driving field is turned on. For this case, we plot the absorption spectrum in Fig.2.

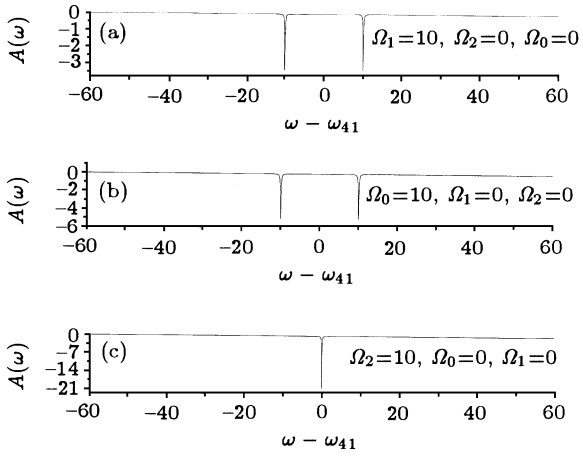


Fig.2. Curve (a): absorption spectra of a weak probe around $1 \to 4$ transmission for Ω_1=10, Ω_0=0, Ω_2=0, $\Delta_1 = \Delta_2 = \Delta_3 = 0$, $\gamma_1 = \gamma_2 = \gamma_3 = \gamma_5 = 0.05$. Curve (b): same as curve (a), except that Ω_1=0, Ω_0=10, $\Omega_2 = 0$. Curve (c): same as curve (a), except that Ω_1=0, Ω_0=0, Ω_2=10.

Figures 2(a) and 2(b) illustrate the typical absorption spectrum. We can explain the above results in the dressed state representation easily. Secondly, we see the situation that there are only two driving fields turned on. The spectrum is shown in Fig.3.

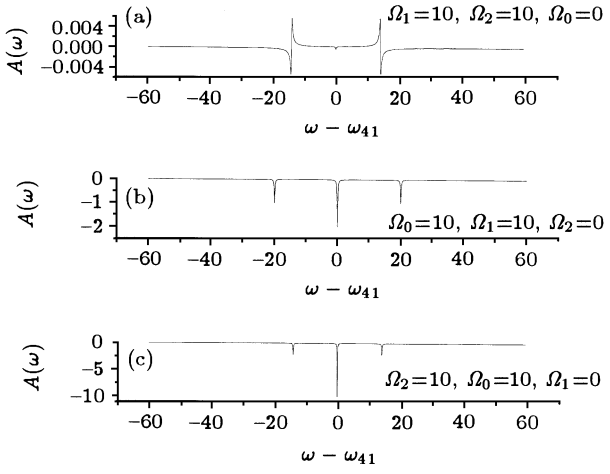


Fig.3. Curve (a): absorption spectra of a weak probe around $1 \to 4$ transmission for Ω_1=10, Ω_0=0, Ω_2=10. Curve (b): same as curve (a), except that Ω_1=10, Ω_0=10, Ω_2=0. Curve (c): same as curve (a), except that Ω_1=0, Ω_0=10, Ω_2=10.

On the basis of the eigenstates of the interaction Hamiltonian (dressed atomic states), we can obtain the eigenvalues of the interaction Hamiltonian for the three cases.

For case (a), Ω_1=10, Ω_0=0, Ω_2=10, E_1=0.0, $E_2 = \sqrt{\Omega_1^2 + \Omega_2^2}$, $E_3 = -\sqrt{\Omega_1^2 + \Omega_2^2}$.

For case (b), Ω_1=10, Ω_0=10, Ω_2=0, $E_1=\Omega_1$, $E_2 = -\Omega_1$, $E_3 = \Omega_0$, $E_4 = -\Omega_0$.

For case (c), Ω_1=0, Ω_0=10, Ω_2=10, E_1=0.0, $E_2 = \sqrt{\Omega_2^2 + \Omega_0^2}$, $E_3 = -\sqrt{\Omega_2^2 + \Omega_0^2}$.

Curves (a), (b) and (c) in Fig.3 illustrate the typical appearance of three spectral components in resonance: one centres at the atomic transition frequency and two symmetric pairs of sidebands separated by $\pm\Omega$ from the centre, where $\Omega = (\Omega_1^2+\Omega_2^2)^{\frac{1}{2}}$ in Fig.3(a) and $\Omega = 2\Omega_0 = 2\Omega_1$ in Fig.3(b) and $\Omega = (\Omega_2^2 + \Omega_0^2)^{\frac{1}{2}}$ in Fig.3(c). From Fig.3, we can also see that the peak heights in the three cases are different from each other. We give an explanation by the population difference of the $1 \to 4$ transition. For case (a), the population in level 4 (ρ_{44}) is approximately equal to the population in level 1 (ρ_{11}), but for $\rho_{44} < \rho_{11}$. For case (b), the population in level 1 (ρ_{11}) is approximately equal to the population in level 2 (ρ_{22}) and $\rho_{11} + \rho_{22} = 1.0$. For case (c), all the population is level 1 ($\rho_{11} = 1.0$). The absorption spectrum of the $1 \to 4$ transition is in direct proportion to the population difference of the $1 \to 4$ transition. So the peak height in case (c) is the maximal ($\rho_{44} - \rho_{11} = -1$) and the peak height in case (a) is minimal ($\rho_{44} - \rho_{11} \approx 0.0$).

The absorption spectrum can be split into two parts:

$$\langle [P^{(-)}(z), P^{(+)}(\tau_0)] \rangle = \hat{\Gamma}(z) = \hat{\Gamma}_1(z) + \hat{\Gamma}_2(z), \quad (17)$$

$$\begin{aligned} \hat{\Gamma}_1(z) &= M_{33}(z)(2\Psi_{15} - 1 + \Psi_5 + \Psi_{10}) \\ &= M_{33}(z)(\rho_{44} - \rho_{11}), \end{aligned} \quad (18)$$

$$\begin{aligned} \hat{\Gamma}_2(z) =& \mu_{41}\mu_{14}(M_{31}(z)\,\Psi_{13} + M_{32}(z)\,\Psi_{14} \\ & - M_{37}(z)\,\Psi_4 - M_{311}(z)\,\Psi_8 - M_{315}(z)\,\Psi_{12}) \\ =& \mu_{41}\mu_{14}(M_{31}(z)\rho_{42} + M_{32}(z)\rho_{43} \\ & - M_{37}(z)\rho_{21} - M_{311}(z)\rho_{31} - M_{315}(z)\rho_{41}). \end{aligned} \quad (19)$$

From the above equations we can also calculate the dependence of the absorption spectrum on the stationary population differences between levels 1 and 4 ($\rho_{44} - \rho_{11}$), in addition to the off-diagonal elements (ρ_{42}, ρ_{43}, ρ_{21}, ρ_{31}, ρ_{41}).

Figure 4 shows the contribution of the populations. The results completely agree with the above analysis given in the dressed states.

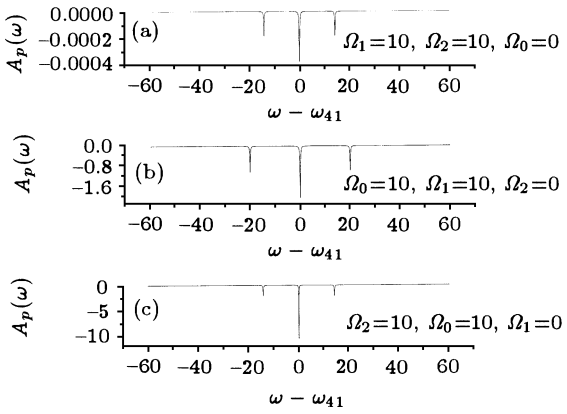


Fig.4. Curve (a): the population contribution to the absorption spectrum of the $4 \to 1$ transition for Ω_1=10, Ω_2=10, Ω_0=0. Curve (b): same as curve (a), except that Ω_1=10, Ω_0=10, Ω_2=0. Curve (c): same as curve (a), except that Ω_1=0, Ω_0=10, Ω_2=10. Other parameters are the same as in Fig.2.

However, so far, the published papers about the absorption spectrum have been limited to the systems driven by two driving fields. Here, we consider the case having three driving fields ($\Omega_0 \neq 0$, $\Omega_1 \neq 0$, $\Omega_2 \neq 0$). We find that there are many differences between the absorption spectrum produced by an atom driven by two and by three resonant fields. Figure 5 illustrates the role of the spectrum in resonance with Ω_1=10, Ω_0=10, Ω_2=10.

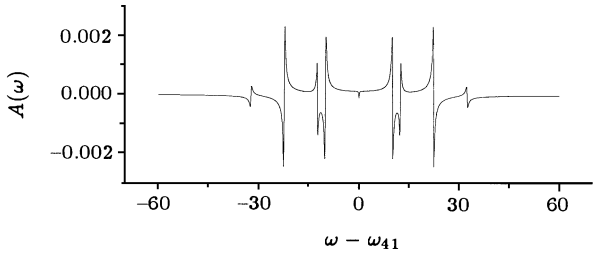


Fig.5. Absorption spectra of a weak probe around the $1 \to 4$ transition. The parameters are Ω_1=10, Ω_2=10, Ω_0=10. Other parameters are the same as in Fig.2.

On the basis of the eigenstates of the interaction Hamiltonian, we can obtain the eigenvalues and eigenstates of the interaction Hamiltonian:

$$E_1 = \sqrt{\frac{(\Omega_1^2+\Omega_2^2+\Omega_0^2)+\sqrt{(\Omega_1^2+\Omega_2^2+\Omega_0^2)^2-4\Omega_0^2\Omega_1^2}}{2}}, \tag{20a}$$

$$E_2 = -\sqrt{\frac{(\Omega_1^2+\Omega_2^2+\Omega_0^2)+\sqrt{(\Omega_1^2+\Omega_2^2+\Omega_0^2)^2-4\Omega_0^2\Omega_1^2}}{2}}, \tag{20b}$$

$$E_3 = \sqrt{\frac{(\Omega_1^2+\Omega_2^2+\Omega_0^2)-\sqrt{(\Omega_1^2+\Omega_2^2+\Omega_0^2)^2-4\Omega_0^2\Omega_1^2}}{2}}, \tag{20c}$$

$$E_4 = -\sqrt{\frac{(\Omega_1^2+\Omega_2^2+\Omega_0^2)-\sqrt{(\Omega_1^2+\Omega_2^2+\Omega_0^2)^2-4\Omega_0^2\Omega_1^2}}{2}}, \tag{20d}$$

$$|\alpha\rangle = (x_1^2|1\rangle + x_2^2|2\rangle + x_3^2|3\rangle + x_4^2|4\rangle)_{E=E_1}, \tag{21a}$$

$$|\beta\rangle = (x_1^2|1\rangle + x_2^2|2\rangle + x_3^2|3\rangle + x_4^2|4\rangle)_{E=E_2}, \tag{21b}$$

$$|\gamma\rangle = (x_1^2|1\rangle - x_2^2|2\rangle + x_3^2|3\rangle - x_4^2|4\rangle)_{E=E_3}, \tag{21c}$$

$$|\varsigma\rangle = (x_1^2|1\rangle - x_2^2|2\rangle + x_3^2|3\rangle - x_4^2|4\rangle)_{E=E_4}, \tag{21d}$$

where

$$x_1 = \frac{1}{1+\left(\frac{E}{\Omega_1}\right)^2+\left(\frac{E^2-\Omega_1^2}{\Omega_1\Omega_2}\right)^2+\left(\frac{\Omega_0(E^2-\Omega_1^2)}{\Omega_1\Omega_2 E}\right)^2}, \tag{22a}$$

$$x_2 = \frac{\frac{E}{\Omega_1}}{1+\left(\frac{E}{\Omega_1}\right)^2+\left(\frac{E^2-\Omega_1^2}{\Omega_1\Omega_2}\right)^2+\left(\frac{\Omega_0(E^2-\Omega_1^2)}{\Omega_1\Omega_2 E}\right)^2}, \tag{22b}$$

$$x_3 = \frac{\frac{E^2-\Omega_1^2}{\Omega_1\Omega_2}}{1+\left(\frac{E}{\Omega_1}\right)^2+\left(\frac{E^2-\Omega_1^2}{\Omega_1\Omega_2}\right)^2+\left(\frac{\Omega_0(E^2-\Omega_1^2)}{\Omega_1\Omega_2 E}\right)^2}, \tag{22c}$$

$$x_4 = \frac{\frac{\Omega_0(E^2-\Omega_1^2)}{\Omega_1\Omega_2 E}}{1+\left(\frac{E}{\Omega_1}\right)^2+\left(\frac{E^2-\Omega_1^2}{\Omega_1\Omega_2}\right)^2+\left(\frac{\Omega_0(E^2-\Omega_1^2)}{\Omega_1\Omega_2 E}\right)^2}. \tag{22d}$$

For simplicity, let $\Omega_1 = \Omega_2 = \Omega_0$ under the resonant condition. Obviously, there are nine components:

$$\begin{aligned} &|\alpha\rangle \to |\alpha'\rangle, |\alpha\rangle \to |\beta'\rangle, |\alpha\rangle \to |\gamma'\rangle, \\ &|\alpha\rangle \to |\varsigma'\rangle, |\beta\rangle \to |\alpha'\rangle, |\beta\rangle \to |\gamma'\rangle, \\ &|\gamma\rangle \to |\alpha'\rangle, |\gamma\rangle \to |\beta'\rangle, |\varsigma\rangle \to |\alpha'\rangle. \end{aligned} \tag{23}$$

Figures 6(a) and 6(b) show the two separate con-

tributions of the populations and coherences to the absorption spectrum.

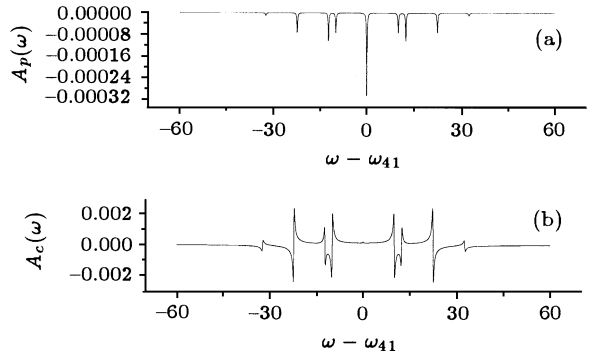


Fig.6. (a) The population contribution [Eq.(18)] to the absorption spectrum of Fig.5. (b) The coherence contribution [Eq.(19)] to the absorption spectrum of Fig.5. The parameters for both (a) and (b) are the same as in Fig.2.

From the figure we can see that the population contribution to the spectrum can only produce absorption, as one would expect in the absence of inversion, while, if gain does develop, it does so by virtue of the atomic coherence.

Finally, we consider the effects of the Doppler broadening on the spectrum. The frequencies of the three fields in the atomic frame should be velocity dependent:

$$\omega_1' = \omega_1(1 - V_y/C), \omega_2' = \omega_2(1 - V_y/C),$$
$$\omega_0' = \omega_0(1 - \eta V_y/C), (\eta = \pm 1), \qquad (24)$$

where V_y is the atomic velocity component along the propagating direction of the field ω_1; $\eta = 1$ refers to the case when ω_0 and ω_1 are co-propagating, while $\eta = -1$ refers to the case when ω_0 and ω_1 are counter-propagating. In the calculation, we keep ω_1 and ω_2 co-propagating. If we replace ω_1, ω_2, ω_0 with ω_1', ω_2', ω_0' in the calculation of the absorption spectrum in Eq.(9), we get an absorption spectrum of the atoms in the atomic coordinates:

$$< \hat{\Gamma}(z) >= \int_{\Delta_1 - 4\omega_D}^{\Delta_1 + 4\omega_D} P(\delta_1)(\hat{\Gamma}(z))\mathrm{d}\delta_1, \qquad (25)$$

where

$$\delta_1 = \Delta_1 + \omega_1 V_y/C, \qquad (26)$$

$$Z = i(\omega - (\omega_{21} + \omega_{32} - \omega_{34}) + (\Delta_1 + \Delta_2 - \Delta_3) + (\delta_1 - \Delta_1) + (\delta_1 - \Delta_1)\omega_2/\omega_1 - \eta(\delta_1 - \Delta_1)\omega_0/\omega_1, \qquad (27)$$

$$P(\delta_1) = \left[\frac{\pi\omega_D^2}{4\ln 2}\right]^{-1/2} \exp\left[\frac{\ln 2(\delta_1 - \Delta_1)^2}{\omega_D^2}\right], \qquad (28)$$

$$\omega_D = \frac{\omega_1}{C}\left[\frac{8KT\ln 2}{M}\right]^{1/2}, \qquad (29)$$

where ω_D is the Doppler broadening. Figure 7 shows the calculated results.

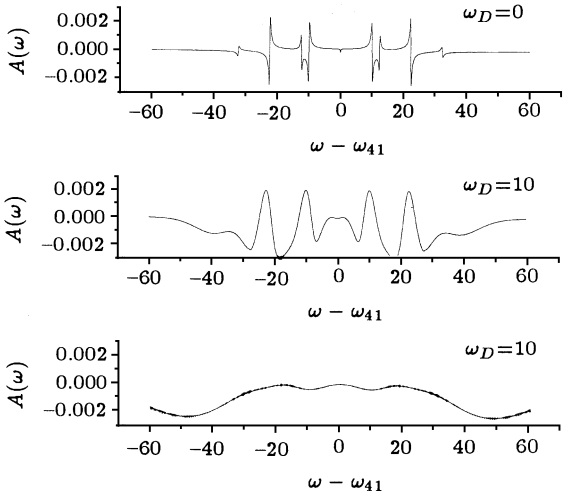


Fig.7. The Doppler effect on the $1 \to 4$ transition for $\Omega_1 = 10$, $\Omega_2 = 10$, $\Omega_0 = 10$; curve (a) represents the spectrum without Doppler broadening; curves (b) and (c), $\omega_D = 10.0$, correspond to the Doppler broadening cases when ω_0 and ω_1 are co- and counter-propagating, respectively.

Figure 7(a) represents the spectrum without Doppler broadening, while Figs.7(b) and 7(c) with $\omega_D = 10.0$ correspond to the Doppler broadening cases when ω_0 and ω_1 are co- and counter-propagating, respectively. From Figs.7(b) and 7(c), we can conclude that when ω_0 and ω_1 are co-propagating, the resolution of the three-driving-field absorption profile is more or less independent of Doppler broadening; i.e., the main feature of the ideal homogeneous case is preserved fairly accurately and gain should be observable even in a cell environment. But in the case when ω_0 and ω_1 are counter-propagating, the Doppler broadening makes the absorption minimum increase and the resolution of the absorption profiles decrease.

By using Eq.(13) we can also discuss the absorption spectra of the other transitions, i.e., $1 \to 2$, $1 \to 3$, $2 \to 3$, $4 \to 3$. The procedure is similar to the analysis of the $1 \to 4$ transition.

In summary, we have studied the steady absorption spectrum of a four-level Doppler-broadened system driven by three coherent fields. The work begins with the calculation of the spontaneous emission

spectrum and is completed with a detailed analysis of absorption properties. In addition to the results of numerical calculation, we provide an explanation about the results in the dressed atomic representation and give an insight into the physical origin of the gain in view of the existence of a population inversion between the levels of the lasing transition. Finally, we explore the effect of Doppler broadening on the absorption profile of a weak probe.

References

[1] Stroud Jr C R 1971 *Phys. Rev.* A **3** 1044

[2] Hartig W and Walther H 1973 *Appl. Phys.* **1** 171

[3] Grove F Y R E and Ezekiel S 1975 *Phys. Rev. Lett.* **35** 1426

[4] Agarwal G S 1970 *Phys. Rev.* A **2** 2038; **4** (1971) 1778

[5] Wineland D J and Itano W M 1981 *Phys. Lett.* A **82** 75

[6] Bergquist J C, Hulet R G, Itano W M and Wineland D J 1986 *Phys. Rev. Lett.* **14** 1699

[7] Narducci L M, Scully M O, Oppo G L, Ru P and Tredicce J R 1990 *Phys. Rev.* A **42** 1630

[8] Manka A S, Doss H M, Narducci L M, Ru P and Oppo G L 1991 *Phys. Rev.* A **43** 3748

[9] Zhu S Y, Narducci L M and Scully M O 1995 *Phys. Rev.* A **52** 4791

[10] Yuan S and Gao J Y 2000 *Eur. Phys. J. D.* **11** 267

[11] Yuan S and Gao J Y 2000 *Chin. Phys.* **9** 436

[12] Mollow B R 1972 *Phys. Rev.* A **5** 2217; Haroche S and Hartmann F ibid **6** 1280